Planck-HFI thermal architecture: from requirements to solutions

Michel Piat, Jean-Michel Lamarre, Julien Meissonnier, Jean-Pierre Torre, Philippe Camus, et al.

Michel Piat, Jean-Michel Lamarre, Julien Meissonnier, Jean-Pierre Torre, Philippe Camus, Alain Benoit, Jean-Pierre Crussaire, Peter A. R. Ade, James J. Bock, Andrew E. Lange, Ravinder Bhatia, Bruno Maffei, Jean Loup Puget, Rashmi V. Sudiwala, "Planck-HFI thermal architecture: from requirements to solutions," Proc. SPIE 4850, IR Space Telescopes and Instruments, (5 March 2003); doi: 10.1117/12.461777

SPIE.

Event: Astronomical Telescopes and Instrumentation, 2002, Waikoloa, Hawai'i, United States

Planck-HFI thermal architecture: from requirements to solutions

Michel Piat[a*], Jean-Michel Lamarre[b], Julien Meissonnier[a], Jean-Pierre˚Torre[c], Philippe Camus[d], Alain Benoit[d], Jean-Pierre Crussaire[a], Peter A.R. Ade[e], Jamie Bock[f], Andrew Lange[g], Ravinder S. Bhatia[g], Bruno Maffei[e], Jean-Loup Puget[a], Rashmi V. Sudiwala[e]

[a] Institut d Astrophysique Spatiale, Orsay, France
[b] LERMA, Observatoire de Paris, France
[c]Service d A ronomie, Verri res le Buisson, France
[d]CRTBT, Grenoble, France
[e]Cardiff University, Wales, UK
[f]Jet Propulsion Laboratory, Pasadena, Ca, USA
[g]Caltech, Pasadena, Ca, USA

ABSTRACT

The Planck-High Frequency Instrument (HFI) will use 48 bolometers cooled to 100mK by a dilution cooler to map the Cosmic Microwave Background (CMB) with a sensitivity of $\Delta T/T \sim 2.10^{-6}$ and an angular resolution of 5 minutes of arc. This instrument will therefore be about 1000 times more sensitive than the COBE-DMR experiment. This contribution will focus mainly on the thermal architecture of this instrument and its consequences on the fundamental and instrumental fluctuations of the photon flux produced on the detectors by the instrument itself. In a first step, we will demonstrate that the thermal and optical design of the HFI allow to reach the ultimate sensitivity set by photon noise of the CMB at millimeter wavelength. Nevertheless, to reach such high sensitivity, the thermal behavior of each cryogenic stages should also be controlled in order to damp thermal fluctuations that can be taken as astrophysical signal. The requirement in thermal fluctuation on each stage has been defined in the frequency domain to degrade the overall sensitivity by less than 5%. This leads to unprecedented stability specifications that should be achieved down to 16mHz. We will present the design of the HFI thermal architecture, based on active and passive damping, and show how its performances were improved thanks to thermal simulations.

Keywords: Sub-millimeter bolometric instrumentation — thermal architecture — thermal stability

1. HFI OVERVIEW

The project Planck[1] of the European Space Agency is intended to be, after COBE and MAP[2], the next generation of Cosmological Microwave Background (CMB) experiments, pushing to its limits the knowledge that will be retrieved from the CMB observation with unprecedented angular resolution and sensitivity. This satellite will survey the sky at sub-millimetre and millimetre wavelengths. Two instruments will share the focal plane of Planck: (i) the Low Frequency Instrument (LFI) using radio detectors and (ii) the High Frequency Instrument (HFI) using Caltech-JPL spiderweb bolometers[3] cooled at 100mK by a space qualified dilution cooler.
The six spectral bands of HFI will cover the frequency range between 100 and 1000GHz with an angular resolution of about 5 minutes of arc and a sensitivity of $\Delta T/T \sim 2.10^{-6}$. As will be seen, the HFI sensitivity will be limited, in the CMB channels, by the statistical fluctuations of the CMB itself, which makes it a kind of ultimate experiment. It will also measure the polarization of the CMB in three channels, giving independent and unique information on the CMB anisotropy[4]. The Planck-HFI mission and objectives are detailed in these proceedings[5].
In this paper, we present the thermal architecture of this instrument and its consequences on the performances.

* michel.piat@ias.u-psud.fr; phone 33 (0)1 69 85 85 77; fax 33 (0)1 69 85 86 75; Institut d Astrophysique Spatiale, B timent 121, Universit Paris Sud, 91405 Orsay France

IR Space Telescopes and Instruments, John C. Mather, Editor,
Proceedings of SPIE Vol. 4850 (2003) © 2003 SPIE · 0277-786X/03/$15.00

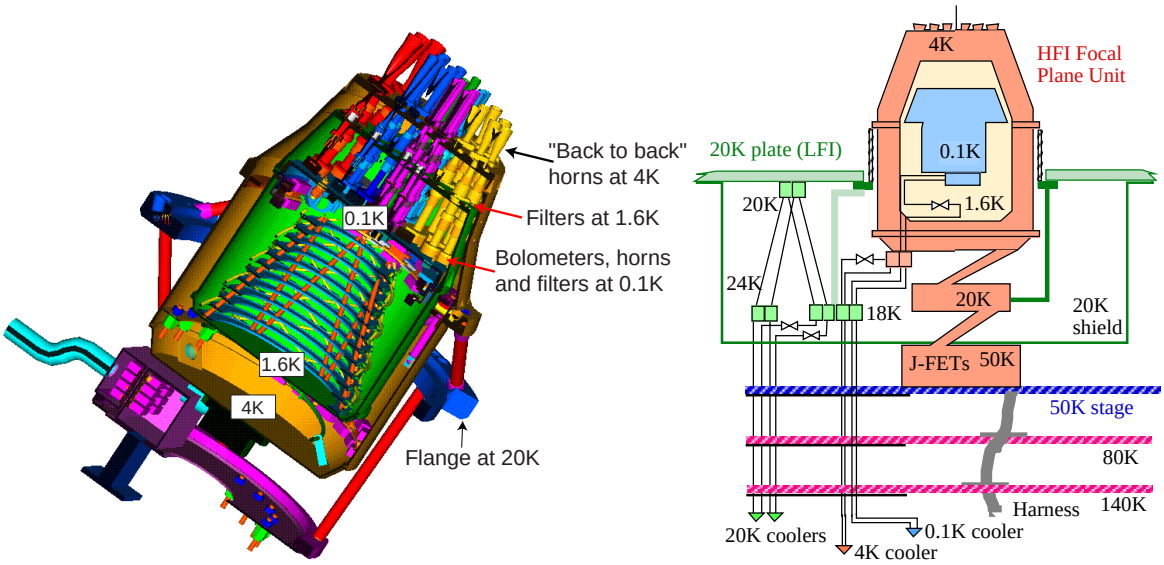

Fig. 1: Left: internal architecture of the HFI Focal Plane Unit. Right: HFI cryogenic architecture.

2. ARCHITECTURE OF THE DETECTOR ASSEMBLY

A major difficulty of high sensitivity submillimetre instruments is to obtain a good optical coupling of the bolometers while insuring a perfect thermal isolation of the coldest stage, including from the radiative point of view. The solution that is used for the HFI is original. A prototype of it has recently been tested with success on the Archeops balloon-borne experiment[6]. The architecture of the detector assembly is represented in Fig. 2.

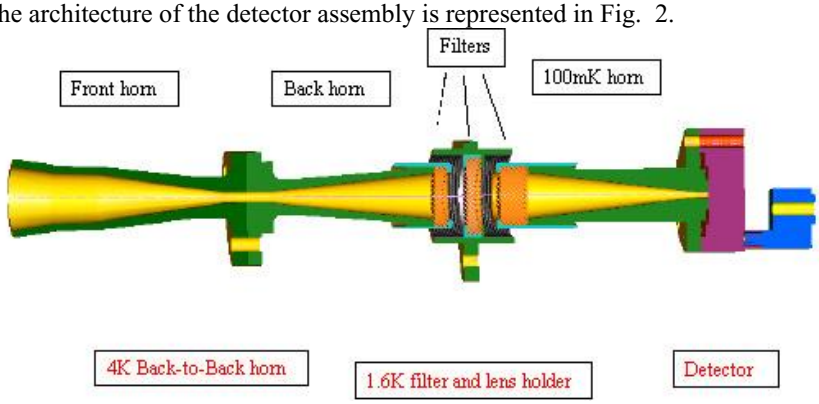

Fig. 2: Detector assembly showing, for each detector, the three horns, the lenses and the filters.

The main feature of this solution is to use three cryogenic stages to damp the thermal radiation by horns and filters while perfectly controlling the optical coupling. The key element is the back to back horn attached on the 4K stage, that permit only to the wanted radiation modes to propagate into the 4K enclosure.

For each detector assembly, filters are used on the three low temperature cryogenic stages (4K, 1.6K, and 0.1K). They are designed to define the bands of each channel and also to provide a proper thermal radiative insulation of the two coldest stages.

The first filter in the chain, situated on the 4K back-to-back horns, should reflect back to the sky as much unwanted high frequency radiation as possible. The 1.6K filter stack is positioned between the back horn and the 100mK horn, where a beam waist defined by the use of two lenses allows to use the filters in a parallel beam. These filters reject

radiation from the higher temperature horns. Finally, the waveguide filter on the 100mK stage rejects longwave power from the 4K horns.

Thus, strategic placement of the filters will enable us to:
- Define the spectral passbands with waveguide filters where appropriate.
- Minimise the thermal loading on the 100mK fridge and 1.6K stage by rejecting short wavelength thermal energy.
- Minimise stray light getting to detectors.
- Maximise the in-band spectral transmission.

3. ULTIMATE SENSITIVITY: THE PHOTON NOISE

The ultimate limitation to the sensitivity of radiometers is the quantum fluctuations of the radiation itself, i.e. photon noise of the flux reaching the detector, ideally only that from the observed source[7]. The High Frequency Instrument (HFI) is designed to approach this ideal limit. The signal to noise ratio obtained by one detector after an integration time t can be given by:

$$\frac{S}{N} = \frac{W_{signal}}{NEP(2t)^{-1/2} + W_{systematics}}$$

where W_{signal} is the power absorbed by the detector, after transmission by the optical system, NEP is the Noise Equivalent Power of the detection system, including intrinsic detector noise, photon noise, and spurious signals and $W_{systematics}$ is the power associated with the part of systematic effects, such as spin synchronous variations of straylight and temperature, that cannot be taken away in the data reduction process.
The various contributors to the background power on the HFI detectors, and therefore to the photon noise, are represented in Fig. 3. The background power originates mainly from the CMB for λ>1.5mm, and mainly from the thermal emission of the telescope at shorter wavelengths. A colder telescope improves the sensitivity at high frequencies. At low frequencies, the HFI is designed to approach the quantum noise of the CMB itself.
The thermal background from the 1.6K and the 4K stages may be limiting factors to the sensitivity of the instrument. Therefore, their temperature must be limited.

An instrument approaching the theoretical limit sensitivity must meet severe requirements in several domains:
(i) The detectors intrinsic noise must be small with respect to photon noise
(ii) The efficiency of the optical system must be high.
(iii) The straylight must have negligible impact on the measurement.
(iv) The time response, the noise spectrum, and the detector layout must be consistent with the sky coverage strategy
(v) In addition, other sources of noise, such as those induced by ionising particles or electromagnetic interference must be kept negligible.

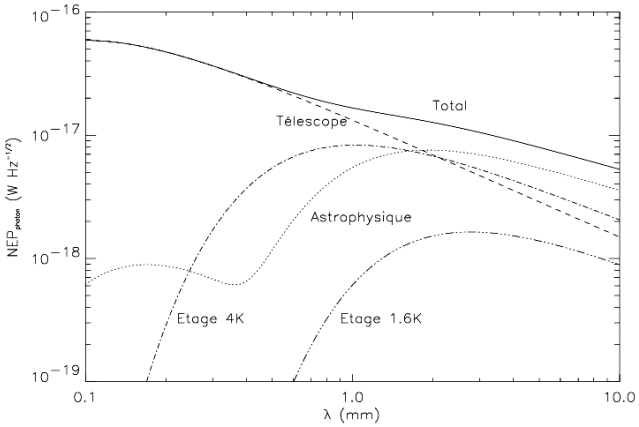

Fig. 3: The power on the detectors originates from internal and external sources that produce contributions to the total photon noise. At low frequencies (long wavelength), photon noise from the CMB itself limits the sensitivity.

4. THERMAL FLUCTUATIONS

4.1 The Planck scanning strategy and its consequences

The whole sky will be covered by scanning it slowly along large circles. The Planck satellite will orbit around the L2 point at a distance of ~1.5 10^6 km from the Earth. It will rotate at 1rpm around its spin axis which will be in antisolar direction. The beam axis, located at about 85¡ from the spin axis, scans the sky along large circles. The spin axis is relocated about every hour so that each circle is scanned about 60 times covering the whole sky on six months.

We can therefore write the measured signal m(t) as the multiplication of a 60 seconds periodic signal s(t) by a top hat function $p_{\Delta t}(t)$ of width Δt equal to about 3600 seconds. In the Fourier space, it is equivalent to convolving the corresponding Fourier transforms:

$$M(f) = S(f) * P_{\Delta t}(f)$$

with $P_{\Delta t}(f) = \Delta t \, sinc(f \, \Delta t)$.

As s(t) is a periodic signal, its Fourier transform is a series, f_{spin} being the spinning frequency (1/60Hz):

$$S(t) = \sum_{k=-\infty}^{+\infty} a_k \, \delta(f - k \, f_{spin})$$

The spectrum of the Planck data is shown schematically in Fig. 4.

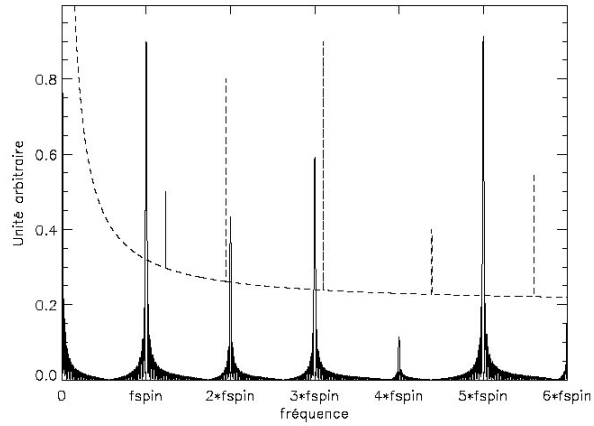

Fig. 4: Example of a realization of the Planck/HFI Signal (solid line) and the noise (dashed line) in the Fourier space (partially represented for convenience).

Each of the components k of the signal is of interest and the a_k will be measured by using an appropriate filter, the simplest one being a sinc function centred on the studied frequencies: $H_k(f) = sinc[\Delta t \, (f - k f_{spin})]$.

As a consequence, the measurement stability must be provided down to 0.01Hz, but only spin-synchronous (or nearly synchronous) fluctuations are detected as a signal.

For example, the readout electronics based on an AC bias associated with a capacitive load does not add low frequency excess noise down to 0.01Hz [8,9].

It has been shown that low frequency noise not correlated with the pointing direction could be removed during post-flight data processing[10]. This is obtain by using data redundancy when the observation strategy produces crossing circles on the sky and in the absence of any other sources of low frequency noise. Nevertheless, a stable instrument assures that scientific results will be available even in the case of partial sky coverage, and the baseline requirement of Planck/HFI is measurement stability down to 0.01Hz.

4.2 Temperature stability requirements

In the space-qualified version of the dilution refrigerator, ^{3}He and ^{4}He are mixed at the junction of two small capillary tubes, which creates a random sequence of ^{3}He concentrated and ^{3}He diluted phases. This succession causes fluctuations of the 0.1K stage temperature that are mainly at low frequencies.

Low frequency fluctuations of the 0.1K stage temperature produce noise on bolometers essentially via conductive coupling. At frequencies used for the measurement, the Noise Equivalent Power (NEP) NEP_T coming by conduction from thermal fluctuations of the 0.1K stage must be less than 30% of the total NEP: $NEP_T < 30\% \, NEP_{tot}$.

This means that we allow an increase of the total NEP of less than 5%, which is a conservative requirement.
The requirement in terms of Amplitude Spectral Density (ASD) of the 0.1K stage temperature is deduced by using the characteristic of the coupling:

$$ASDT = \frac{NEP_T}{\frac{\partial W}{\partial T}} < \frac{30\% NEP_{tot}}{\frac{\partial W}{\partial T}}$$

where the coupling factor is the dynamic conductance of the bolometer:

$$\frac{\partial W}{\partial T} = G - \frac{\alpha R I^2}{T}$$

G is the static conductance of the bolometer, α is the dimensionless sensitivity of the bolometer, R its resistance, I the bias current and T the temperature.
This approach applied to HFI leads to the requirement ASDT < 19 nK.Hz$^{-0.5}$ for the 100mK stage that supports the bolometers.
For spin induced fluctuations which have a line spectrum, it is more convenient to compare the RMS value:

$$T_{RMS} < \frac{0.3}{\sqrt{\Delta t}} \frac{NEP_{tot}}{\frac{\partial W}{\partial T}} = \frac{0.3}{60} \frac{NEP_{tot}}{\frac{\partial W}{\partial T}}$$

This leads to $T_{RMS} < 0.32nK$.

4.3 100mK stage thermal architecture

The main sources of temperature fluctuations on the 100mK bolometer plate are the dilution itself and background radiation fluctuations. An estimated damping factor of about 5000 is needed to stabilize the system. To damp temperature fluctuations, a thermal architecture has been defined, using a passive thermal filters to remove high frequency fluctuations and an active control that suppress low frequency components. Such systems have been tested successfully[11] on the Symbol cryostat which is a test bench for HFI sub-systems. The principle to realize such thermal architecture is summarized with the 3 following rules[12]:

1. Control all thermal paths between sources of temperature fluctuations and point to stabilize (filters, horns)
2. Active control in the thermal path to allow long period stability
3. Low pass filtering to remove artifacts of the active system and to allow short term stability.

Fig. 5 is a support for the description of the various elements used for the HFI 100mK thermal architecture and of their interconnection.
The mechanical support of the heat exchanger consists of struts of Niobium-titanium alloy and of plateaux used to thermalize the heat exchanger tubes and the wiring (the number of plateaus is not properly represented on Fig. 5).
The counterflow heat exchanger is thermally connected to all plateaus except for the coldest one (the dilution plate). It goes directly from the last but one plateau (at 105mK) to the dilution exchanger. The dilution exchanger (dilution on the drawing) is a cylinder around which the dilution tubes are wound. Part of this cylinder consists of high heat capacity material (to damp high frequency thermal fluctuations at the source) through which it is attached to the PID1 box. The PID1 box is a hollow Nb-Ti alloy cylinder (a good thermal isolator at 100mK) implementing the mechanical support of the dilution and PID1 assembly. This system is described in the next section. Its function is to actively damp near to the source the fluctuations induced by the dilution.
The Dilution plate supports the PID1 box, the wiring and the connectors needed for the PID1.
The wiring runs along the mechanical support. At contact with the dilution plate, bunches of 7 wires are put in a flat arrangement and thermalized on the plate. Part of it stops at the dilution plate while most of it goes to the connector s plate. The part of the wiring from the dilution plate to the connector s plate is thermally linked to continuous or distributed pieces of Holmium (Ho foil on the drawing) in order to damp thermal fluctuations propagated through the wires.
YHo struts are the high heat capacity supports of the upper part. They implement a very efficient passive filtering[13] as shown on Fig. 7.
The Connectors plate insures the interface with the bolometer s plate and supports the connectors. It can be in principle in any material provided that the proper thermal links are implemented from the YHo struts to the bolometer s plate.
PID2 insures the control of the absolute temperature of the bolometer s plates and compensate for very slow fluctuations induced by external sources such as cosmic rays or background radiation fluctuations.

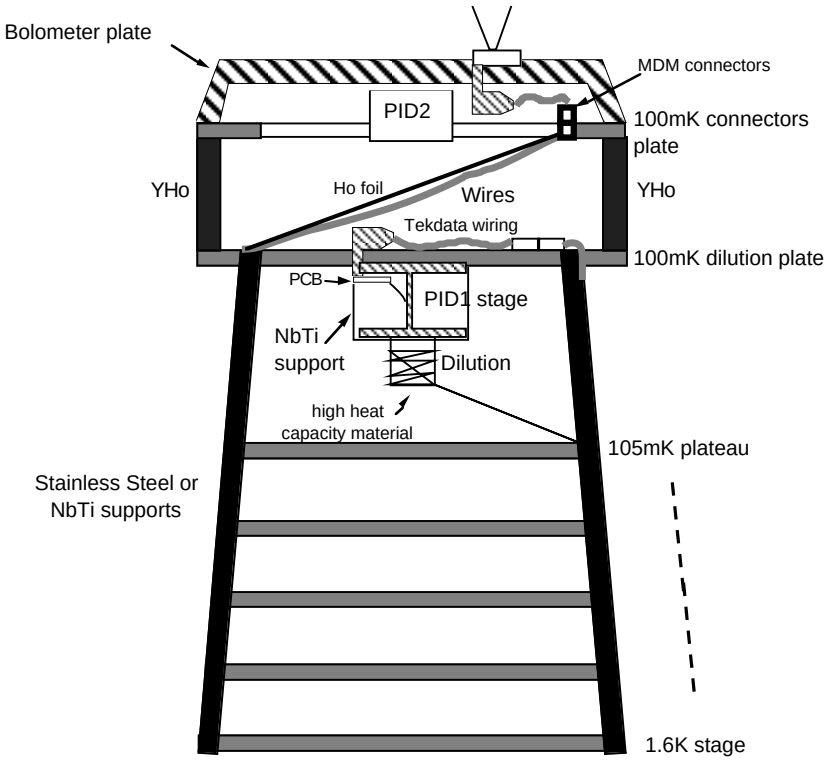

Fig. 5: Schematic view of the 100mK stage thermal control architecture (not to scale).

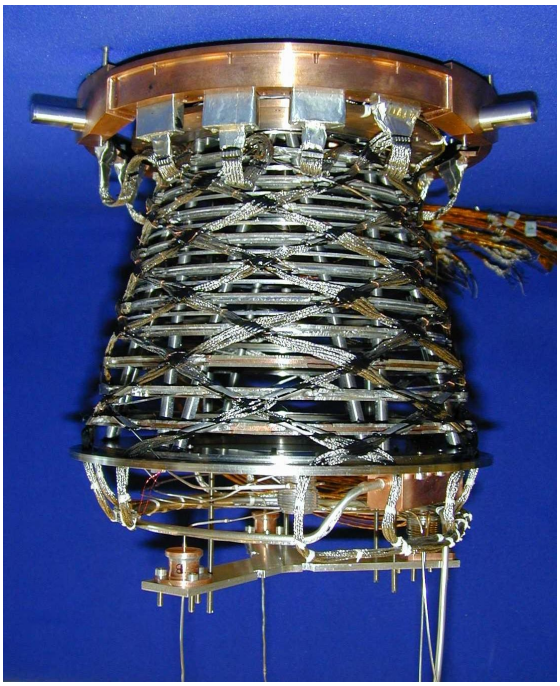

Fig. 6: Breadboard model of the Planck-HFI 100mK heat exchanger realised by Air Liquide.

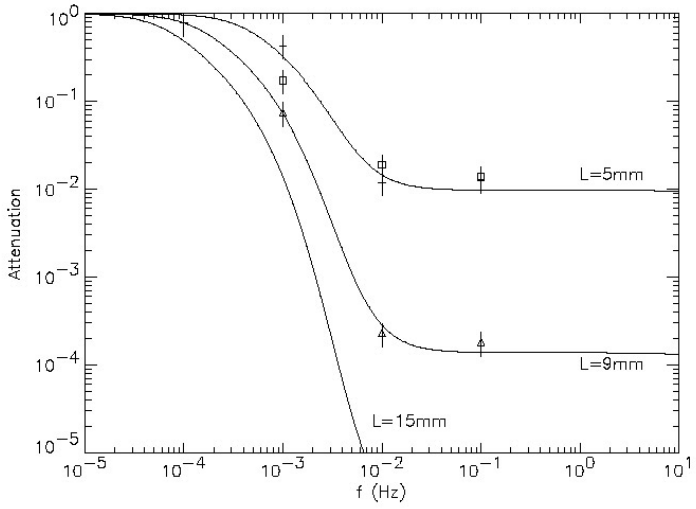

Fig. 7: The points represents the measured damping factor in temperature for different lengths of a YHo sample as a function of frequency. The solid line is the best fit from a model[13].

4.4 Optimization of the active control PID1 system

The active control system PID1 is shown on Fig. 8a. Its mechanical support is obtained thanks to a NbTi hollow cylinder while the thermal link is realized by a Cu link. At low temperature (below about 1K), NbTi become a superconductor and the thermal conductivity between the dilution plate and the dilution itself is dominated by the thermal link. The connection between the thermal link and the two interfaces is done with two Cu arms that absorb differential thermal dilatation. The temperature used for the input of the regulation algorithm is measured with an optimized NTD Ge thermometer from Haller-Beeman[14,15].

In quasi-static regime, we can consider that the regulation system is perfect ($\delta T_{regul}=0$) and the transfer function of the system is similar to a divider bridge in electronics:

$$\frac{\delta T_{dil\ plate}}{\delta T_{dil}} = \frac{R_{link}}{R_{link}+R_{support}}$$

where R_{link} and $R_{support}$ are the thermal resistances of the Cu link and of the mechanical support respectively. In the case of the PID1 system, the quasi static damping factor is theoretically higher than 2000.

In order to optimize this subsystem, a model has been realized with IDEAS and thermally simulated with the TMG module. This model is shown on Fig. 8b.

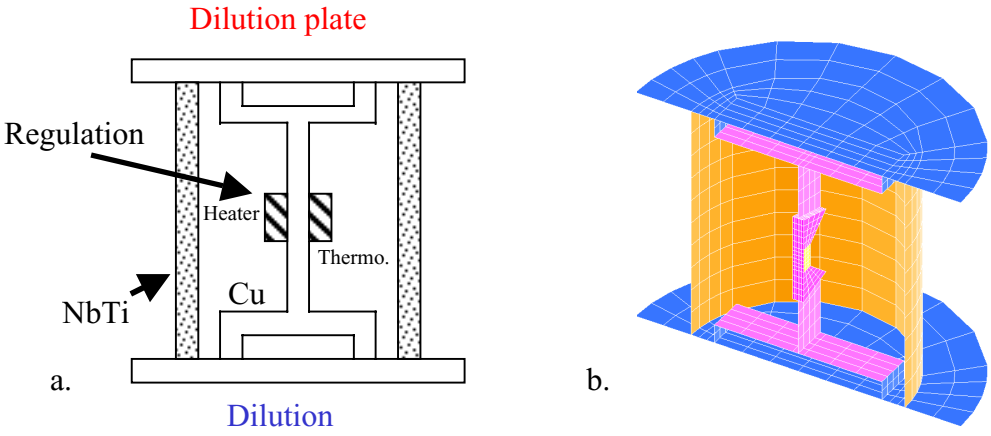

Fig. 8: a : Principles of the PID1 thermal control system. b: Cut-off view of the IDEAS-TMG PID1 model. This system realize the active control of the HFI 100mK thermal architecture.

In order to have realistic simulations, a real PID algorithm was added to the simulation by the way of a Fortran routines. This procedure use the temperature measured by the thermometer (averaged on its surface) to adjust the dissipated power on the heater. The regulation algorithm (which is a PID for Proportional Integral and Derivative) has been duplicated from the one used on the Symbol experiment.

First, these simulations allow us to optimize the thermal gradients that appear in the thermal link. This is the first principle determined experimentally: to suppress as much as possible all thermal paths that bypath the thermometer-heater regulation system. As shown on Fig. 8b, this leads to decrease the width of the thermal link where the thermometer-heater system is placed.
Nevertheless, with this first optimization step, the damping factor was limited to some 10 as shown in the blue curves of Fig. 9. This was due to important thermal gradients between the heater and the cold part of the system that are seen by the thermometer directly placed in front of the heater.
By placing the thermometer in a part of the thermal link where thermal gradients are lower, we get a damping factor of more than 2000, limited in this case by the finite resolution of the simulation.

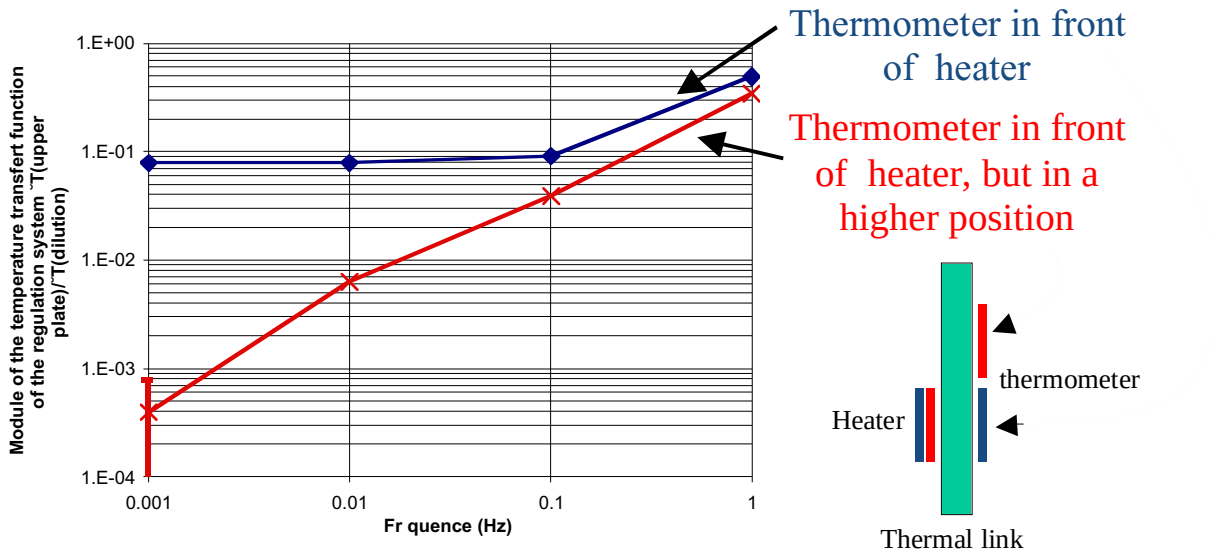

Fig. 9: Transfer function of the simulated PID1 system.

5. CONCLUSIONS

We have shown that the thermal architecture of the Planck-HFI allow to reach the ultimate sensitivity set by the photon noise of the CMB at millimeter wavelength. Nevertheless, thermal fluctuations of the coolers could induce substantial noise to the data, especially if perturbations are in the useful frequency band covering the range from 10mHz to about 100Hz. Dedicated thermal control architecture have therefore been designed to cope with this problem, especially at 100mK. These systems are based on a combination of a passive filtering and an active regulation system that allow to reach the required stability at high and low frequencies respectively. Thermal simulations have been used to optimize such architecture at 100mK and are currently being used for the 1.6K and 4K stages. The first test of this optimization will begin in September.

REFERENCES

1. ESA/Planck Web site: http://astro.estec.esa.nl/SA-general/Projects/Planck
2. M. Halpern and D. Scott, Astro-ph/9904188
3. J. Bock et al., Proc. *30th ESLAB Symp. Submillimetre and Far-Infrared Space Instrumentation* , 24-26 September 1996, Noordwijk, The Netherlands, ESA SP-388, 119-122, 1996.

4. F.R. Bouchet, J.L. Puget, J.M. Lamarre, *School of Les Houches,* 2000, pp. 103-220
5. J. M. Lamarre et al., *these proceedings*.
6. A. Benoit et al., 2002, *Astroparticle Physics* 17, 101-124.
7. J.M. Lamarre et al., *Space Science Reviews*, 74, 27-36, 1995.
8. Gaertner S. et al. 1997, *Astron. Astrophys., Suppl. Ser*., 126, 151-160.
9. Piat M. et al. 1997, *Proc. 7th Int. Workshop on Low Temperature Detectors LTD-7*, 27 July — 2 August 1997, Munich, Germany, pub. by MPI Physik, ISBN 3-00-002266-X.
10. J. Delabrouille,1998, *PhD thesis univ. Paris XI*.
11. M. Piat et al, 2000, *Proc. 8th Workshop on Low Temperature Detectors LTD-8*, NIMA˚444, 413-418.
12. M. Piat, 2000, *PhD thesis univ. Paris XI*.
13. K. Madet et al., 2002, submitted to *Cryogenics*.
14. M. Piat et al., 2001, *JLTP*, Vol.125, Nos. 5/6.
15. M. Piat et al. 2002, *Proc. 9th Workshop on Low Temperature Detectors LTD-9*, AIP Conference Proceeding Series, 605, 79-82.